Research Square

Preprints are preliminary reports that have not undergone peer review.
They should not be considered conclusive, used to inform clinical practice,
or referenced by the media as validated information.

Critical slowing down at the neuromuscular junction: an early-warning framework for amyotrophic lateral sclerosis

Michael Nolan- Dickinson

michael_nolan32@outlook.com

Independent Researcher https://orcid.org/0009-0000-0083-0352

Research Article

Keywords: reinnervation, dynamical systems, early-warning signals, critical slowing down, motor unit number index, single-fibre electromyography

Posted Date: August 11th, 2026

DOI: https://doi.org/10.21203/rs.3.rs-10642034/v1

License: This work is licensed under a Creative Commons Attribution 4.0 International License.
Read Full License

Additional Declarations: The authors declare no competing interests.

Abstract

Objective. In amyotrophic lateral sclerosis (ALS), disease is monitored largely through accumulated loss. We develop the hypothesis that the stability of the compensation offsetting that loss carries an earlier signal than the level of loss itself, readable as a critical-slowing-down (CSD) signature from instability measures already recorded serially.

Methods. We set out a two-tier framework. Tier 1 treats the joint trajectory of single-fibre electromyography (SFEMG) jitter and fibre density as a coupling between instability and compensation, analysed with a multivariate early-warning estimator. Tier 2 is an immediately runnable screen on existing serial motor unit number index (MUNIX) and compound muscle action potential (CMAP) cohorts, analysing the directly measured signals rather than the derived motor unit size index (MUSIX) ratio, and benchmarking the dynamical metric against CMAP slope under a pre-registered plan. Two generative simulations support the design: a division-artefact analysis with measurement noise fixed to published reliability, and a feasibility analysis of detection power under realistic sparse sampling.

Results. With biological fluctuation held flat, serial variance analysis of MUSIX manufactured a spurious rising-variance signature (relative variance rising ~4.7-fold toward the transition), conditional on the MUNIX measurement floor, and large enough to swamp the effect being sought. Within-patient detection of a planted CSD signal was at chance (area under the curve 0.52–0.56). Stage-aligned cohort-level detection was recoverable but noise-limited, requiring on the order of 80–160 patients at well-standardised noise and underpowered at worst-case noise.

Conclusions. The framework is hypothesis-generating; its most likely outcome on real data is a pre-registered null, itself informative, whereas a positive Tier 2 result would be novel and would discriminate the underlying transition type.

Significance. This is the first application of critical slowing down to the neuromuscular junction — a cheap, retrospective test on existing serial electrophysiology, for which measurement standardisation, not data collection, is the rate-limiting step.

Highlights

● In ALS, the stability of compensation may signal decline earlier than the level of loss.

● Critical slowing down, validated in seizures, is applied for the first time to the NMJ.

● Serial variance analysis of the derived MUSIX ratio can manufacture a spurious early-warning signal.

● A simulation shows cohort-level detection is feasible; within-patient detection is at chance.

1. Introduction

Two well-supported bodies of work sit adjacent to one another without intersecting. The first concerns the neuromuscular junction (NMJ) in ALS, which fails early: denervation and reinnervation proceed as a continuous, asynchronous process that propagates outward from the first lost junction, beginning before frank axonal degeneration [1]. This instability is quantified routinely — through single-fibre electromyography (SFEMG) jitter, impulse blocking, and motor-unit-potential variability, or “jiggle” [2] — and has been for decades.

The second concerns critical slowing down (CSD), a generic statistical signature by which dynamical systems approaching a tipping point recover more slowly from perturbation and show rising autocorrelation and variance in their fluctuations [3]. In neural tissue this is not speculative: CSD has been validated as a biomarker of seizure susceptibility in long-term intracranial recordings [4] and shown to govern the transition of neurons into spiking [5]. The toolkit demonstrably works on neural time-series; it has not been pointed at the periphery — at the junction whose instability is already being recorded.

The closest prior application of this class of method to a neurodegenerative disease is in Parkinson’s disease, where a computational framework modelled progression of the subthalamo-pallidal circuit as approach to a Hopf bifurcation and reported that cross-correlations between state variables provide earlier warning than variance-based CSD indicators [6]. That work is theoretical, is built on a central oscillatory circuit that would require high-precision invasive recording, and concerns a Hopf rather than a fold/saturation transition. The present framework differs in three respects: it targets the peripheral NMJ rather than a central oscillator; it proposes analysis of instability measures clinics already record serially, requiring no new recording modality; and it treats a fold-versus-saturation transition, for which univariate variance and lag-1 autocorrelation are the primary indicators. We nonetheless adopt the central methodological lesson of that work — that near non-fold transitions a multivariate, cross-correlation-based estimator can outperform univariate CSD — in the design of Tier 1 (Section 4).

This paper sets out a framework for crossing that gap, is explicit about the conditions under which the idea is and is not testable, and reports simulations establishing both a measurement artefact any analysis must avoid and the scale of data any real test would require. It reports no new empirical data and makes no clinical claim; its contribution is the framework, its substrate analysis, and the two computational results.

2. Hypothesis

The premise is that the stability of compensation is a more informative early signal than the level of loss. Stated as a single falsifiable claim: in ALS, instability at the NMJ is held in check by reinnervation until a tipping point at which compensation can no longer absorb it; that transition is preceded by a CSD signature — rising autocorrelation and variance — in the appropriate junctional measure, and this dynamical signature predicts subsequent decline better than the static level of the same measure. The hypothesis has two substrates with materially different statistical properties, treated separately below.

3. Bifurcation versus saturation: a risk to the premise and the discrimination it affords

Critical slowing down is not a property of anything that declines. It belongs to systems approaching a fold (saddle-node) bifurcation, where the recovery rate from perturbation falls toward zero as a control parameter crosses threshold. The biology here may instead be resource saturation: reinnervation fails because surviving axons exhaust the supply of denervated fibres available for adoption [7], and a depleting resource reaching a ceiling produces the same rise-then-turnover in compensation without a vanishing recovery rate — and so need not produce any early-warning precursor. It is not known which regime governs reinnervation exhaustion, and CSD exists only for the former. A null therefore carries two meanings — the signal is too small to detect, or the transition is not of the precursor-bearing type — and any honest analysis must report it that way.

The converse is the useful part. Saturation produces the turnover without a rising-autocorrelation precursor; a fold bifurcation produces both. A clean autocorrelation-and-variance rise localised to the pre-turnover window is therefore itself positive evidence for the bifurcation reading, so the analysis discriminates between the two transition types rather than merely being threatened by them. A second-order caution: ALS is increasingly modelled as a spreading process, so a whole-muscle trajectory may reflect a denervating front arriving in that muscle's motor pool rather than a local transition, which would also accelerate loss without local critical slowing.

4. Tier 1: the conceptual test — jitter–fibre-density coupling

The hypothesis takes its cleanest form in single-fibre EMG, and a coupling is genuinely required here because of a specific confound. Increased jitter in ALS has two causes that are indistinguishable at a single time point: a junction approaching failure, and a newly reinnervated, immature junction transmitting unreliably. Jitter alone cannot separate them. Fibre density resolves the ambiguity, because it independently indexes reinnervation: the SFEMG guidelines read the two jointly, treating rising fibre density with settling jitter as successful reinnervation, and rising fibre density with persistent high jitter and blocking as failing compensation that signals rapid progression [8]. Jitter and fibre density are separately measured and not algebraically linked — they share an electrode and motor units, so are not fully independent, but neither is constructed from the other — so their joint trajectory is a true coupling. The early-warning hypothesis is that this coupling destabilises before structural collapse. Because Tier 1 is intrinsically a two-channel coupling, its dynamical readout is specified as a multivariate early-warning estimator — the cross-correlation and time-irreversibility between the jitter and fibre-density series — benchmarked against the univariate variance and lag-1 autocorrelation of each channel, rather than treating the two channels as independent series [cf. 6].

The empirical anchor is real and subclinical. A single-fibre EMG study correlating SFEMG parameters with functional status in ALS examined one limb and two facial muscles — extensor digitorum, frontalis, and orbicularis oculi — and found jitter, blocking, and fibre density significantly abnormal relative to

reference values in all muscles, with the strongest correlations when jitter and fibre density were considered together; it identified a notable ALS Functional Rating Scale–Revised (ALSFRS-R) value close to 30–31 across muscles (31 in extensor digitorum and frontalis, 30 in orbicularis oculi), below which the percentage of increased jitter was higher while fibre density remained relatively low — a candidate transition from successful to failing compensation, although cross-sectional, inferred across patients at differing severities rather than tracked within individuals [9]. An independent single-fibre EMG study of clinically preserved facial muscles reported impaired neuromuscular transmission in ALS, consistent with early, pre-symptomatic junctional involvement [10].

The limitation of this tier is methodological, not merely logistical. Classical fibre density requires the dedicated single-fibre electrode, but the field has largely moved to disposable concentric-needle jitter recording, which does not yield classical fibre density. The current standard method therefore supplies only one of the two channels this tier requires; a study would need the older single-fibre electrode or a validated concentric-needle surrogate for the compensation channel. This is the arm that requires generating purpose-built serial data, ideally in the preserved facial-muscle window the cross-sectional anchor identifies.

5. Tier 2: the immediately runnable screen — directly measured single-channel dynamics

MUNIX (motor unit number index) and CMAP (compound muscle action potential) amplitude have been recorded serially in hundreds of ALS patients [11–13], making this the substrate that can be analysed retrospectively today. It must be analysed with one arithmetic fact in view.

The motor unit size index, MUSIX, is a derived ratio: MUSIX = CMAP ÷ MUNIX. As a dynamical channel it is doubly disqualified. First, it is algebraically locked to MUNIX (MUNIX × MUSIX = CMAP), so any coupling between them is partly definitional, and the entanglement propagates into the variances and covariances a dynamical analysis reads. Second, and decisively, MUNIX declines toward its noise floor as disease advances, and the variance of a ratio whose denominator approaches zero inflates super-linearly from the arithmetic alone — manufacturing exactly the rising-variance-approaching-the-transition signature being sought, with no biology in it, in precisely the window of interest. A CMAP baseline does not protect against this, because the artefact lives in the MUSIX channel specifically. Section 6 quantifies this artefact directly, since the exclusion it justifies is load-bearing for the whole tier.

This framework therefore does not analyse MUSIX. The dynamical test runs on the directly measured signals — CMAP and MUNIX — with CMAP amplitude as the explicit baseline to beat. The pre-registered question is whether the dynamical metric on MUNIX predicts subsequent decline better than the CMAP slope already does. This makes the design self-adjudicating against the standing critique that MUNIX is largely CMAP-driven [14, with reply 15]: if MUNIX dynamics are a degenerate reflection of CMAP, the screen returns null by construction; if they carry independent information, they beat CMAP.

A positive Tier 2 result must be interpreted with care. A single-channel analysis of MUNIX asks whether the loss channel shows critical slowing — a real and novel question, but not the stability-of-compensation thesis, which requires two separately measured channels and survives only in Tier 1. Tier 2's honest role is therefore a go/no-go gate: a null below the CMAP baseline is a strong prior against investing in purpose-built jitter/fibre-density data collection, whereas a positive result licenses it. Winning Tier 2 leaves the central hypothesis untested, by design.

5.1 Analysis specification

For Tier 2, per muscle: detrend the slow decline in CMAP and MUNIX and test whether the lag-1 autocorrelation and variance of the MUNIX residuals rise as the turnover is approached. The detrending method must be pre-specified — for example, a Gaussian-kernel smoother of stated bandwidth, or first differencing — and shown, on the null models below, not to inject residual curvature near a turnover that would itself inflate variance. Stage alignment across patients must use an axis independent of the analysed channel — the ALSFRS-R or time from onset — rather than a staging index derived from the same MUNIX decline, to avoid circularity between the alignment axis and the outcome.

Four nulls must be cleared: a surrogate-data null preserving each series' trend and spectrum; the measurement-noise floor; a division-artefact null that propagates measured CMAP and MUNIX session-to-session noise through the ratio, quantifying how much apparent MUSIX-variance rise that alone produces and thereby demonstrating why MUSIX is excluded (realised in Section 6); and a MUNIX-floor null confirming that the changing measurement variance as MUNIX approaches its floor does not itself generate a spurious rising-variance signature on the channel actually analysed. The dynamical metric must additionally beat the CMAP slope as a predictor of subsequent decline, and a true negative is handled by pre-specified equivalence testing.

The power analysis requires a between-patient random-effects term: patients differ at the same disease stage, that heterogeneity grows near the transition — a substantial fraction of muscles never mount a detectable reinnervation response [11] — and stage-dependent heterogeneity can manufacture a rising-variance signal under the null that no measurement-noise floor removes.

6. The MUSIX division artefact, quantified

6.1 Rationale and model

Section 5 excluded MUSIX on the grounds that a ratio whose denominator approaches its noise floor manufactures a rising-variance signature from arithmetic alone. Because that exclusion is load-bearing for the whole Tier 2 design, we quantify it directly rather than asserting it. That a ratio's variance inflates as its denominator approaches zero is a general statistical fact; the contribution here is to quantify it specifically for MUSIX under measured ALS electrophysiology noise, in the disease window where it bites.

We built a generative model of the three channels across a disease-stage axis, with true MUNIX declining from a normal value (~ 150 index units) toward its floor (~ 15) and true CMAP preserved early and declining later, so that true MUSIX rises as reinnervation enlarges surviving units — the expected biology [11, 12]. Onto the true trajectories we layered measurement noise fixed to published reliability: multiplicative session-to-session noise at a CMAP coefficient of variation (CoV) of 15% [17] and a MUNIX CoV of 14% [18], an additive MUNIX noise floor (the physical basis of "approaching the noise floor"), and a correlation between the CMAP and MUNIX errors, because MUNIX is itself computed from CMAP so their errors partly cancel in the ratio — the mechanism by which MUSIX can appear more reliable than MUNIX in mid-range [16]. Crucially, the biological fluctuation was held flat across stage: there is no critical slowing down in the model, so any stage-dependent rise in observed variance is pure measurement artefact. The model reproduces a mid-stage MUSIX CoV of ~ 16%, within the observed 7.8–28.4% range [16], before being asked to do anything else. Full code, parameters and a parameter sweep are deposited (Supplementary S2, S3; Data and code availability).

6.2 Results

Under the flat-biology null, the relative variance (variance ÷ mean²) of observed MUSIX rose ~ 4.7-fold from early to late stage, whereas directly measured CMAP stayed essentially flat (Fig. 1). The rise is arithmetic, not biological.

Two findings sharpen the claim, and both cut against a naive version of it. First, directly measured MUNIX is not immune: its relative variance also rose (~ 2.4-fold) as it neared its own floor, so the correct statement is that the ratio roughly doubles a floor problem that also touches MUNIX, while CMAP — furthest from its floor — is the cleanest channel. Second, the artefact is conditional on the additive noise floor: with purely multiplicative noise the ratio's relative variance is essentially constant across stage (fold-change ~ 1.0), and it is only as the denominator's absolute noise becomes non-negligible near the floor that the first-order ("relative noise is constant") approximation fails and the variance inflates super-linearly (Fig. 2). The magnitude scales with the floor (Supplementary S3) and, at plausible values, exceeds the CSD effect the feasibility analysis plants (Section 7): on MUSIX, the artefact would swamp the signal being sought.

Finally, because the artefact is white measurement noise, it inflates variance while diluting lag-1 autocorrelation, whereas genuine critical slowing raises autocorrelation. A rising variance accompanied by falling autocorrelation is thus a fingerprint of the artefact rather than of a transition (Fig. 3) — though at four to six serial samples this separates groups, not individuals, consistent with the within-patient result in Section 7.

This is the quantified basis for analysing CMAP and MUNIX directly and excluding the MUSIX ratio, and it supplies the division-artefact null specified in Section 5.1.

7. Feasibility analysis

7.1 Methods

To establish the scale of data any real test would require, and whether the two objections most likely to be raised — large measurement noise and sparse serial sampling — are fatal, we implemented a generative simulation; the full code is openly available (Supplementary S2). Each synthetic patient has a latent disease-stage axis and a compensation signal that rises then turns over at a transition. In “CSD” patients the biological fluctuation variance around the trend rises as the transition approaches (the early-warning signature); in “stable” patients it stays flat. Multiplicative measurement noise is added at the reported MUSIX CoV, for which single-subject round-robin studies report intra-rater values up to approximately 28% [16]. Two detection strategies were tested: one within a single patient’s sparse series, and one across a stage-aligned cohort with the known measurement-noise floor subtracted. Figure 4 shows the detection problem: with six samples at 28% noise, CSD and stable trajectories are difficult to separate by eye.

7.2 Results

Result 1 — within-patient detection is at chance. Separating CSD from stable patients using the variance of one sparse, noisy series performed at chance (area under the curve ≈ 0.52–0.56 at 5, 8, or 12 timepoints, 28% noise). With this measurement noise and this few samples, no within-patient early-warning readout survives. This negative result is robust: it does not depend on the assumed size of the planted signal, because chance performance is chance regardless. The naive within-patient version of the hypothesis should be abandoned.

Result 2 — cohort-level detection is recoverable but noise-limited. Pooling patients by disease stage, estimating residual variance per stage bin, and subtracting the expected measurement-noise variance recovered the rising-variance signature with controlled false-positives (~ 5%). The required cohort size depended sharply on measurement quality (Fig. 5): at ~ 15% CoV, roughly 80–160 patients reached 80% power; at worst-case 28% CoV, even several hundred patients remained underpowered. The decisive variable is measurement noise, not sample size per se — which points to measurement standardisation, rather than data collection, as the rate-limiting step.

7.3 What is real and what is assumed

The constraints are real (28% and 15% CoV, and 4–6 timepoints, from the published reliability and trial literature; cohort sizes in the low hundreds). The size of the CSD signal is assumed, with no empirical anchor, and the power figures scale directly with it: a real effect half as large would roughly quadruple the required sample size, and if no such effect exists, no cohort suffices. The one validated neural CSD system, seizures, shows the signature is subtle and cycle-modulated, which suggests the assumed effect may be optimistic and the power figures a ceiling rather than an estimate. The feasibility simulation establishes plausibility and an order-of-magnitude sample size, not a result; it predates the refined Tier 2 design and does not yet implement the CMAP-slope benchmark or the between-patient

random effect, so its power figures should be read as a sketch pending that update, while the within-patient negative result stands independently. The division-artefact null it originally lacked is now provided by Section 6. A full account of what is real and what is assumed, with the parameter table and power table, is given in Supplementary S1.

8. Limitations

Beyond the bifurcation-versus-saturation ambiguity (Section 3), four limitations define the work. Between-patient heterogeneity is the dominant real-world nuisance and is not removed by subtracting a measurement-noise floor, so any sample-size figure lacking a random-effects term is optimistic. The MUSIX entanglement and its division artefact are handled by analysing CMAP and MUNIX directly and excluding the ratio — and are now quantified rather than merely asserted (Section 6), including the honest boundary condition that the artefact is contingent on the MUNIX noise floor and that MUNIX itself is not perfectly clean near end-stage. The strongest cross-sectional anchor — the ALSFRS-R ≈ 30 inflection — is cross-sectional and does not establish a within-patient transition. And critical slowing down is contested even where best studied: no critical slowing was found before human seizures in one major analysis [19], so a null is a genuine and reportable outcome. The honest prior for a real Tier 2 analysis is null or weak-positive.

9. Conclusion

The instinct underlying this framework — that the stability of compensation may carry earlier information than the level of loss — is testable, and the data to begin testing it largely already exist. The contribution here is to make the test honest: to separate the conceptually clean but data-poor arm (jitter–fibre-density coupling) from the data-rich but constrained arm (single-channel MUNIX dynamics against a CMAP baseline); to confront the MUSIX division artefact and quantify it rather than fall into it; to frame the runnable screen as a go/no-go gate rather than a confirmation; and to establish by simulation that within-patient detection is infeasible while cohort-level detection is feasible at a quantified, noise-dependent scale. The most likely real-world outcome is a pre-registered null with a sharpened understanding of why — itself worth reporting, and a clean gate on the decision to invest in definitive data. We invite re-analysis of existing serial electrophysiology cohorts and collaboration on the purpose-built single-fibre arm.

Declarations

Declaration of competing interest. The author declares no competing interests.

Funding. This research received no specific grant from any funding agency in the public, commercial, or not-for-profit sectors.

Ethics. This work reports no new human or animal data. Both simulations use synthetic data generated in software, and no patient-identifiable information is used.

Data and code availability. The division-artefact simulation (musix_artefact.py), the feasibility simulation (munix_csd_sim.py), the figure script (make_figs.py), all figures, and a full parameter sweep (sensitivity_table.csv) are available via the Open Science Framework (https://osf.io/edqju). All simulations are deterministic given fixed random seeds; every number and figure reproduces exactly (Supplementary S2).

Use of generative artificial intelligence. During the preparation of this work the author used generative AI tools to assist with literature search, drafting, and adversarial self-critique. All scientific judgement, verification of sources, and final responsibility rest with the author; AI-generated hypotheses were treated as requiring independent verification, and only peer-reviewed, citable sources are relied upon for empirical claims.

Scope statement. This is a hypothesis-generating methodological framework. It makes no individual diagnostic or prognostic prediction and provides no clinical guidance; all signals discussed are group-level.

References

1. Martineau É, Di Polo A, Vande Velde C, Robitaille R (2018) Dynamic neuromuscular remodeling precedes motor-unit loss in a mouse model of ALS. eLife 7:e41973. https://doi.org/10.7554/eLife.41973
2. Stålberg E, Sonoo M (1994) Assessment of variability in the shape of the motor unit action potential, the jiggle, at consecutive discharges. Muscle Nerve 17:1135–1144. https://doi.org/10.1002/mus.880171003
3. Scheffer M, Bascompte J, Brock WA, Brovkin V, Carpenter SR, Dakos V et al (2009) Early-warning signals for critical transitions. Nature 461:53–59. https://doi.org/10.1038/nature08227
4. Maturana MI, Meisel C, Dell K, Karoly PJ, D'Souza W, Grayden DB et al (2020) Critical slowing down as a biomarker for seizure susceptibility. Nat Commun 11:2172. https://doi.org/10.1038/s41467-020-15908-3
5. Meisel C, Klaus A, Kuehn C, Plenz D (2015) Critical slowing down governs the transition to neuron spiking. PLoS Comput Biol 11:e1004097. https://doi.org/10.1371/journal.pcbi.1004097
6. Yan H, Coughlin C, Smolin L, Wang J (2024) Unraveling the complexity of Parkinson's disease: insights into pathogenesis and precision interventions. Adv Sci 11:2405309. https://doi.org/10.1002/advs.202405309
7. Dantes M, McComas A (1991) The extent and time course of motoneuron involvement in amyotrophic lateral sclerosis. Muscle Nerve 14:416–421. https://doi.org/10.1002/mus.880140506
8. Sanders DB, Kouyoumdjian JA, Stålberg EV (2019) Single fiber electromyography and measuring jitter with concentric needle electrodes (Guidelines for single fiber EMG). Clin Neurophysiol 130:1417–1439. https://doi.org/10.1016/j.clinph.2019.04.005

9. Rostás R, Fekete I, Horváth L, Márton S, Fekete K (2024) Correlation of single-fiber electromyography studies and functional status in patients with amyotrophic lateral sclerosis. Open Med 19:20240990. https://doi.org/10.1515/med-2024-0990
10. Watanabe K, Kuwabara S, Higashihara M, Sonoo M et al (2022) Impaired neuromuscular transmission in facial muscles of amyotrophic lateral sclerosis: a single-fiber EMG study. Neurol Clin Neurosci 10:78–82. https://doi.org/10.1111/ncn3.12580
11. Chan Y, Alix JJP, Neuwirth C et al (2022) Reinnervation measured by the motor unit size index is associated with preservation of muscle strength in ALS, but not all muscles reinnervate. Muscle Nerve 65:203–210. https://doi.org/10.1002/mus.27444
12. Nandedkar SD, Barkhaus PE, Stålberg EV (2010) Motor unit number index (MUNIX): principle, method, and findings in healthy subjects and in patients with motor neuron disease. Muscle Nerve 42:798–807. https://doi.org/10.1002/mus.21824
13. Ebersbach T, Roediger A, Steinbach R et al (2023) MUNIX loss of 50% occurs in half the time of 50% functional loss: the D50 model. Sci Rep 13:3981. https://doi.org/10.1038/s41598-023-30871-x
14. Bostock H, Jacobsen AB, Tankisi H (2019) Motor unit number index and compound muscle action potential amplitude. Clin Neurophysiol 130:1734–1740. https://doi.org/10.1016/j.clinph.2019.05.031
15. Nandedkar SD, Barkhaus PE, Stålberg EV (2019) Motor unit number index (MUNIX) and compound muscle action potential amplitude: a reappraisal. Clin Neurophysiol 130:2010–2011. https://doi.org/10.1016/j.clinph.2019.07.021
16. Alix JJP, Neuwirth C, Gelder L et al (2019) Assessment of the reliability of the motor unit size index (MUSIX) in single-subject round-robin and multi-centre settings. Clin Neurophysiol 130:666–674. https://doi.org/10.1016/j.clinph.2019.02.009
17. Kong X, Lesser EA, Gozani SN (2009) Repeatability of nerve conduction measurements derived entirely by computer methods. Biomed Eng Online 8:33. https://doi.org/10.1186/1475-925X-8-33
18. Neuwirth C, Burkhardt C, Alix JJP, Castro J, de Carvalho M, Gawel M et al (2016) Quality control of motor unit number index (MUNIX) measurements in 6 muscles in a single-subject round-robin setup. PLoS ONE 11:e0153948. https://doi.org/10.1371/journal.pone.0153948
19. Wilkat T, Rings T, Lehnertz K (2019) No evidence for critical slowing down prior to human epileptic seizures. Chaos 29:091104. https://doi.org/10.1063/1.5122759

Figures

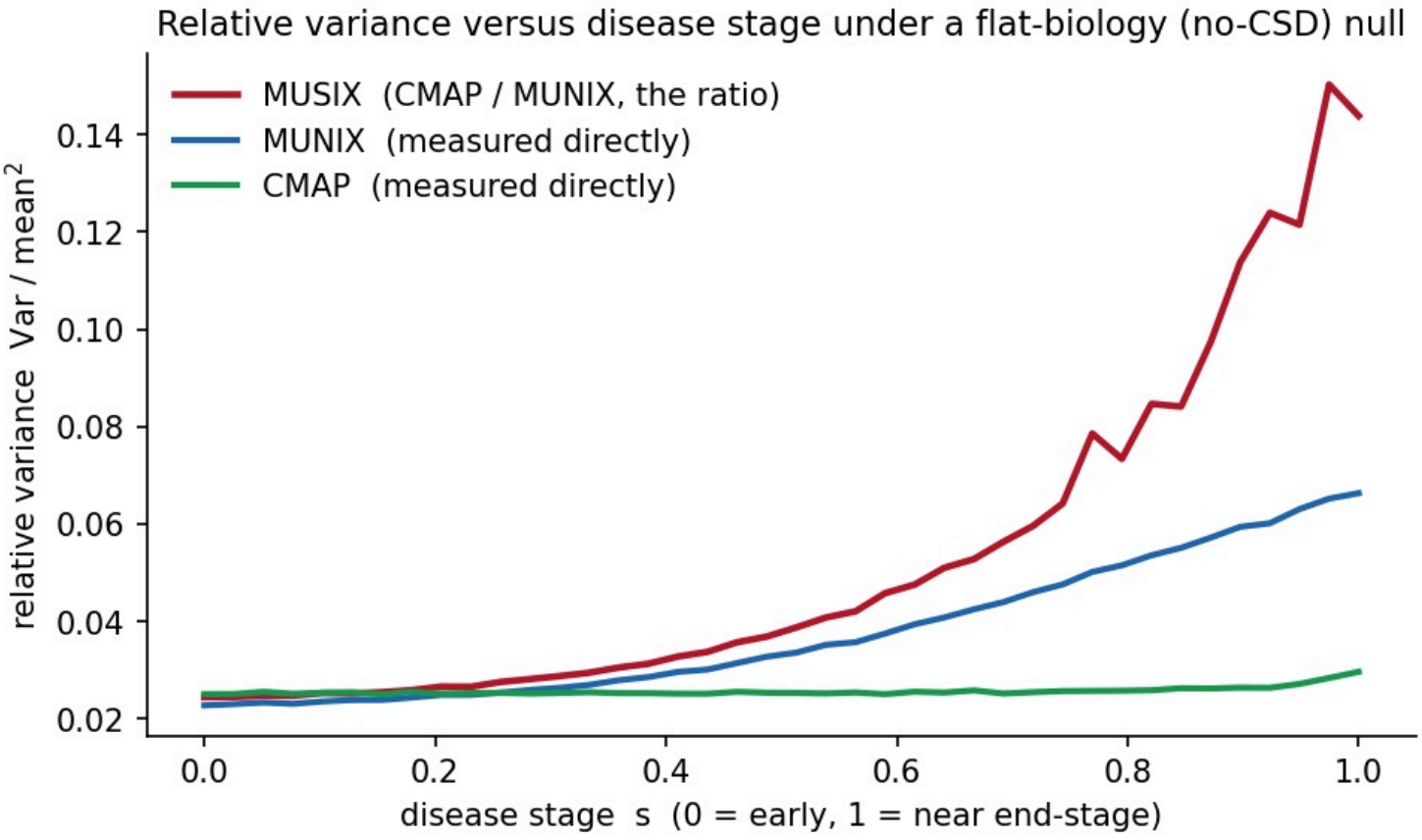


Figure 1

Relative variance (variance / mean^2) of observed CMAP, MUNIX and MUSIX across the disease-stage axis under a flat-biology null (no critical slowing down). Measurement noise is fixed to published reliability (CMAP CoV 15% [17], MUNIX CoV 14% [18], an additive MUNIX floor, error correlation rho = 0.6). With biology held constant, MUSIX (the ratio) shows a ~4.7-fold rise toward the transition and MUNIX a ~2.4-fold rise as each nears its floor, while CMAP stays flat. The MUSIX rise is arithmetic, not biological.

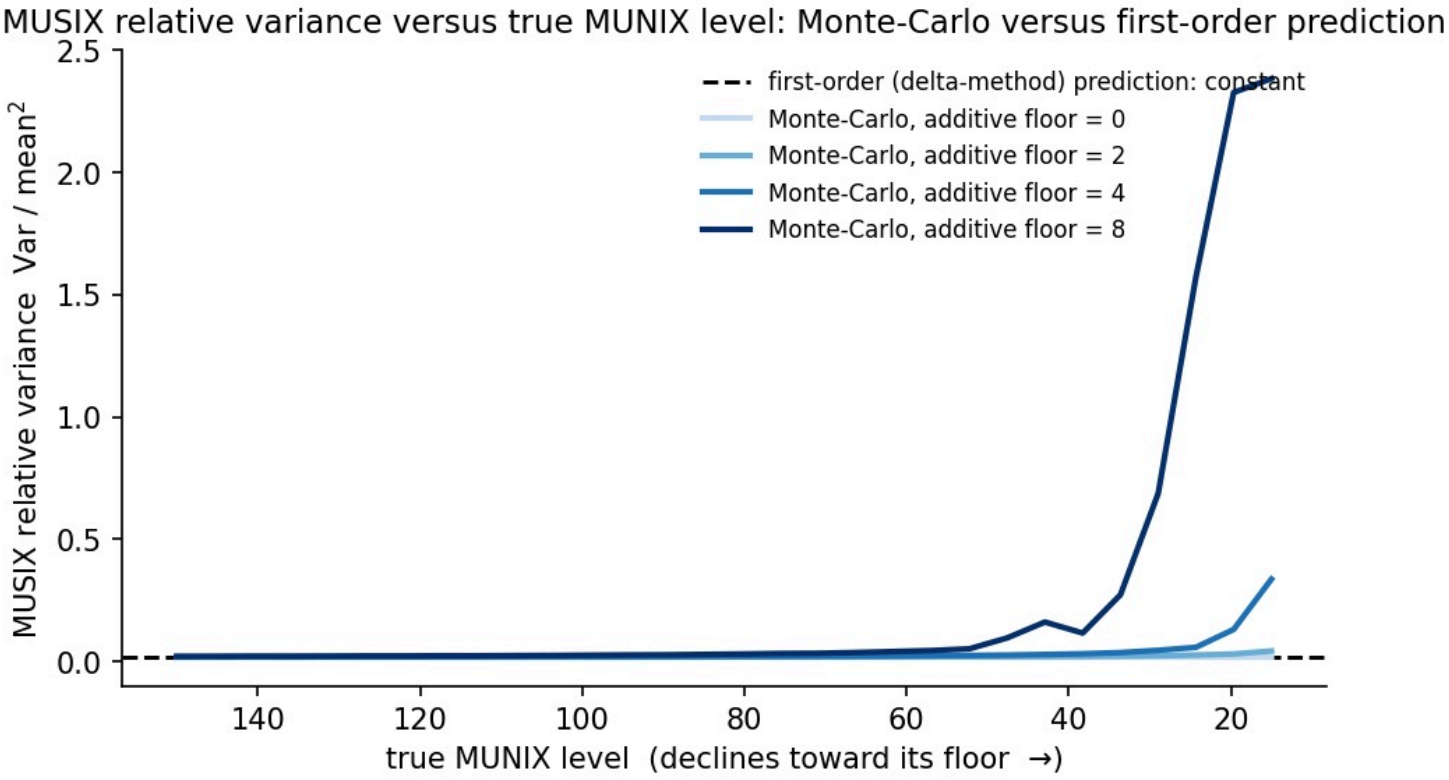


Figure 2

MUSIX relative variance as a function of the true MUNIX level (disease progresses as MUNIX falls, rightward), for several additive-noise-floor magnitudes, compared with the first-order (delta-method) prediction (dashed), which is constant. The Monte-Carlo variance tracks the constant prediction until MUNIX approaches its floor, then inflates super-linearly; the inflation scales with the additive floor and vanishes when it is zero.

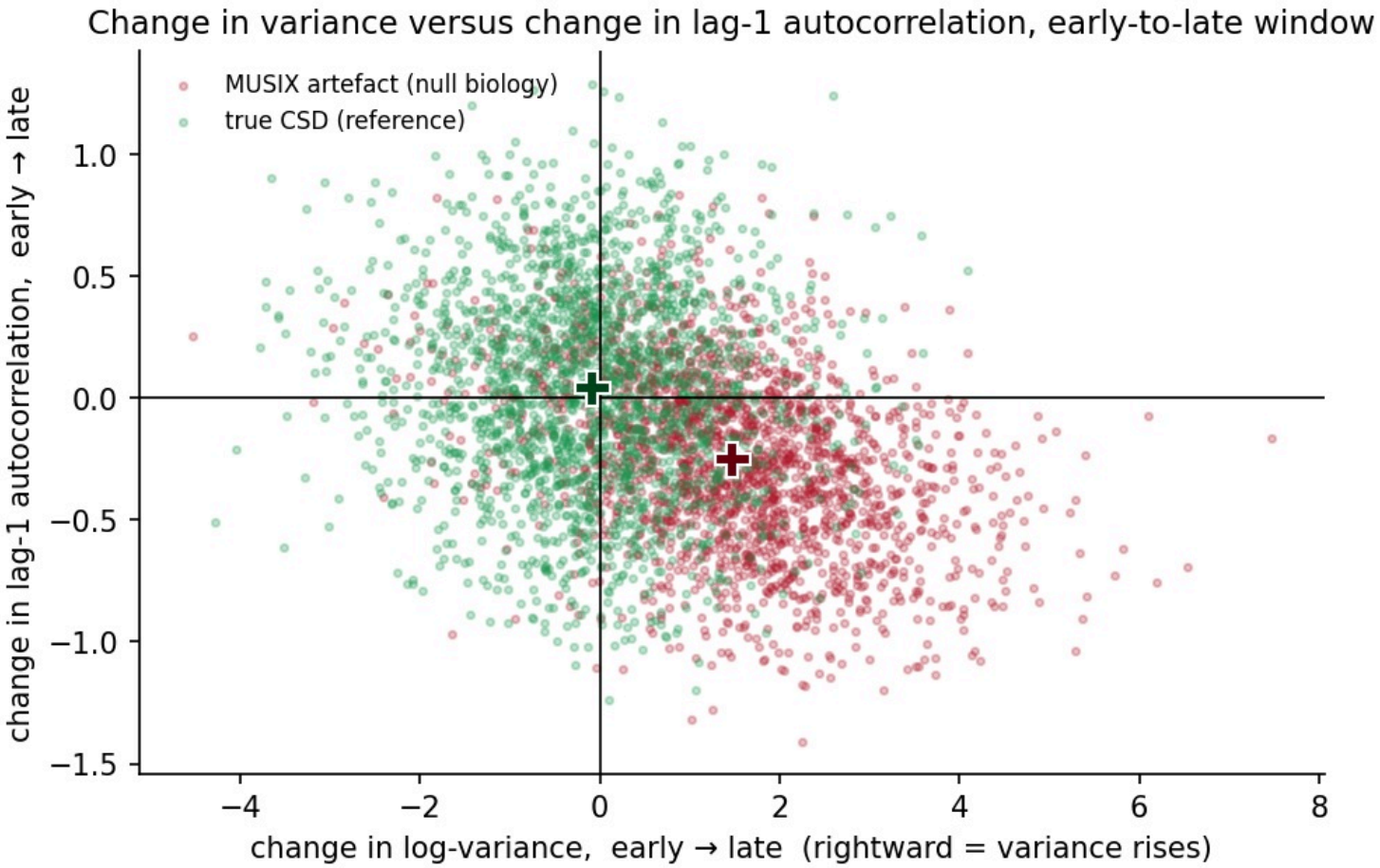


Figure 3

Change in log-variance versus change in lag-1 autocorrelation from an early to a late serial window (six timepoints), for the MUSIX artefact channel (flat biology) and a reference channel with genuine critical slowing down. The artefact raises variance while lowering autocorrelation (lower right); true CSD raises autocorrelation. Crosses mark medians. The heavy overlap shows the separation is group-level, not per-patient.

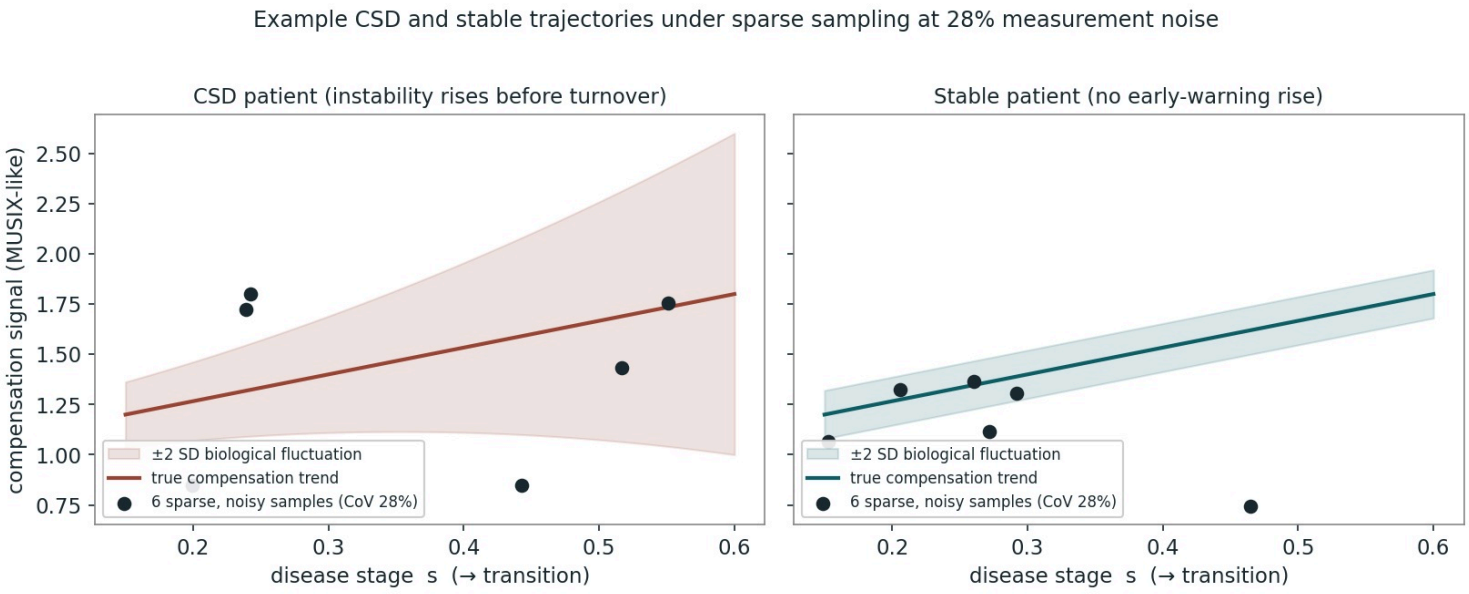


Figure 4

The detection problem. A rising-variance early-warning signature versus a stable trajectory, each shown with the true compensation trend, the +/-2 SD biological-fluctuation band, and six sparse samples at 28% measurement noise. The two are hard to distinguish from sparse, noisy data.

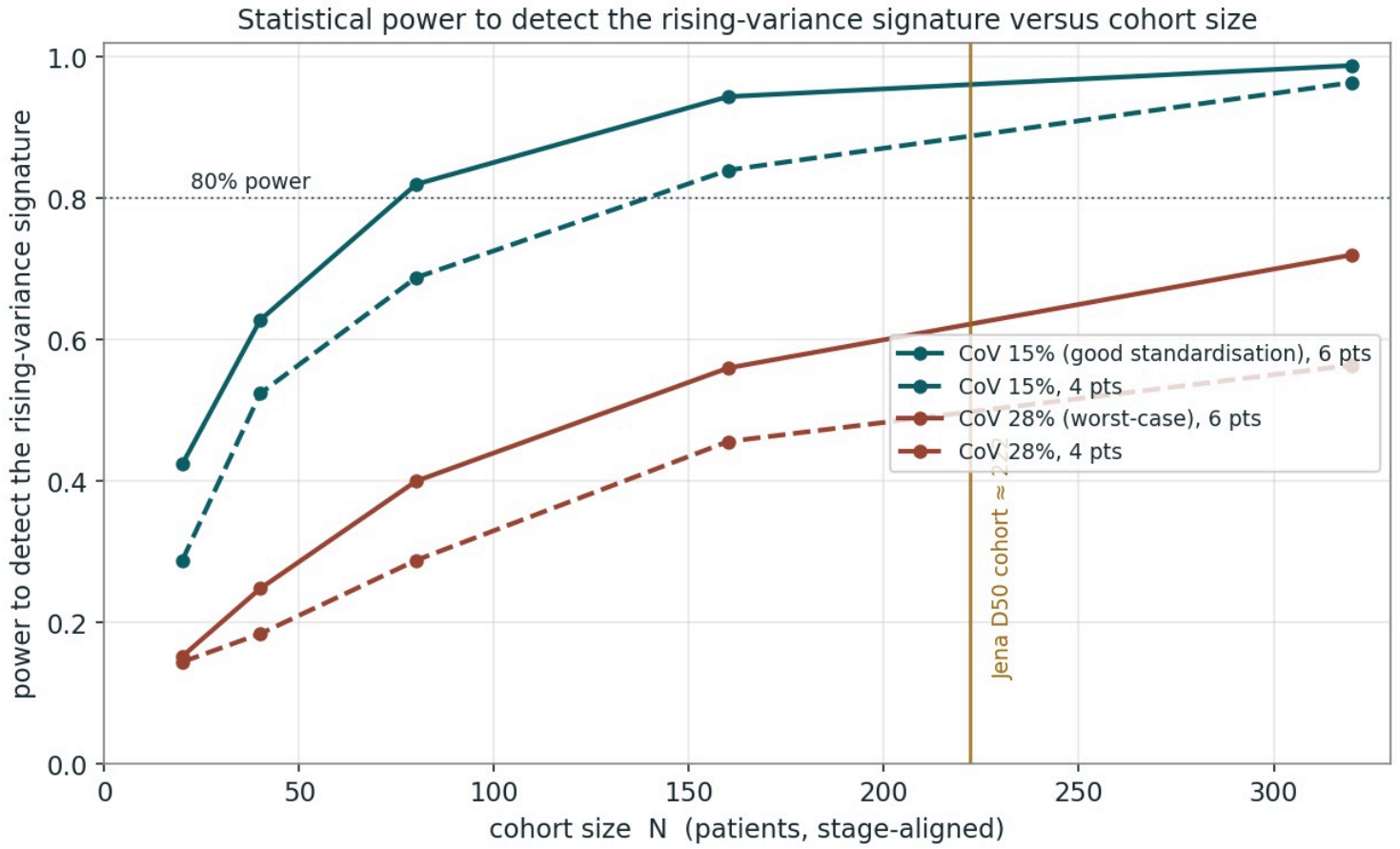


Figure 5

Cohort-level recoverability. Statistical power to detect the rising-variance signature versus cohort size, at two measurement-noise levels (15% and 28% CoV) and two sampling densities (4 and 6 timepoints). The dotted line marks 80% power; the vertical marker shows a representative existing cohort size (~222).

Supplementary Files

This is a list of supplementary files associated with this preprint. Click to download.

- SupplementaryMaterial.docx